Homodyne Reconstruction and IDEAL (Dixon) Water-Fat Decomposition

S. B. Reeder[1], B. A. Hargreaves[2], H. Yu[1,2], J. H. Brittain[3]

[1]Radiology, Stanford University, Stanford, California, United States, [2]Electrical Engineering, Stanford University, Stanford, California, United States, [3]Applied Science Lab-West, GE Healthcare, Menlo Park, California, United States

Introduction: Reliable separation of water from fat using "Dixon" approaches has received renewed interest in recent years as it provides uniform separation of water from fat despite the presence of B_o and B_1 field inhomogeneities (1). Homodyne reconstruction is commonly used to reconstruct partial *k*-space acquisitions, exploiting the Hermitian symmetry of *k*-space in order to maximize spatial resolution (2) and reduce scan time. Unfortunately, conventional homodyne methods demodulate the phase information from source images. This phase is required to decompose water from fat using "Dixon" methods. Previous results using "Dixon" with partial k-space acquisitions have reconstructed images by filling unsampled portions of *k*-space matrices with zeroes. This approach preserves phase, but will cause moderate blurring.

In this work, we describe the integration of homodyne reconstruction with an Iterative Dixon water-fat separation with Echo Asymmetry and Least squares estimation (IDEAL) method (3,4). Using this combination, resolution of calculated water and fat images can be maximized for partial *k*-space acquisitions.

Theory: The signal from a pixel at position ***r*** containing magnetization from water (W) and fat (F) acquired at discrete echo times t_n (n=1,…, N), in the presence of field inhomogeneity, $\psi(r)$ (Hz), can be written,

$$s_n(r) = \left(|W(r)|e^{i\phi_W(r)} + c_n|F(r)|e^{i\phi_F(r)}\right)d_n(r) \qquad (1)$$

where the relative chemical shift of fat relative to water is Δf_{fw} (-210Hz at 1.5T), $c_n = e^{i2\pi\Delta f_{fw}t_n}$ and $d_n = e^{i2\pi\psi(r)t_n}$. If the field map, $\psi(r)$, is known, then d_n(r) can be demodulated from eq. 1 and water and fat are easily decomposed in the least squares sense (3). If $d_n(r)$ is unknown, an iterative method can be used to calculate the field map, and water and fat subsequently separated (3).

Similar to conventional homodyne reconstruction, the first step of the combined homodyne-IDEAL reconstruction is to filter the sampled *k*-space data with a symmetric low pass filter $G_L(k)$ (2), and perform the Fourier transform to obtain images that have low resolution in the undersampled direction, $\hat{s}_n(r) = \mathcal{F}\{S_n(k)G_L(k)\} = s_n(r) * g_L(r)$ **(2)**

Assuming that the field map, $\psi(r)$, is smoothly varying, a good estimate of the field map, $\hat{d}_n(r)$, can then be made using the iterative approach (3). In addition, low-resolution estimates of the phase of water ($\hat{\phi}_W(r)$) and fat ($\hat{\phi}_F(r)$) images can be calculated, and these terms can be used below to demodulate the phase maps of the final water and fat images, as is done with conventional homodyne reconstruction (2). Next, the sampled data is filtered with a ramp transition or step function filter, $G_R(k)$, such that

$$\tilde{s}_n(r) = \mathcal{F}\{S_n(k)G_R(k)\} = \left((W(r) + c_nF(r))d_n(r)\right) * g_R(r) \qquad (3)$$

Figure 1: Cropped coronal images of IDEAL-FSE T2W images of the knee of a normal volunteer, using partial ky acquisition, reconstructed with a) full resolution, b) zero-filling and c) proposed homodyne method.

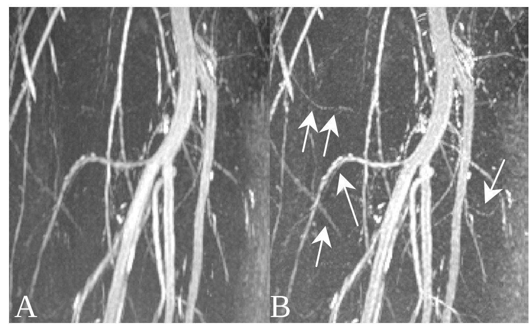

Figure 2: Cropped MIP images of IDEAL-SSFP non-contrast enhanced images of popliteal trifurcation acquired with partial readout, reconstructed with a) zero-filling and b) proposed homodyne method. Arrows show improved resolution.

If it can be assumed that the field map is smoothly varying such that $d_n(r)$ varies only slightly over the width of $g_R(r)$, similar to the assumptions made by Noll *et al* for phase maps (2), $d_n(r)$ can be brought through the convolution, ie:

$$\tilde{s}_n(r) \approx \left(W(r) * g_R(r) + c_nF(r) * g_R(r)\right)d_n(r) = \left(\tilde{W}(r) + c_n\tilde{F}(r)\right)d_n(r) \qquad (4)$$

Assuming $\hat{d}_n(r) \approx d_n(r)$, d_n(r) is demodulated from equation 4, and estimates of filtered water and fat images are made with least-square method (3), such that, $\tilde{W}(r) = |W(r)|e^{i\phi_w(r)} * g_R(r) \approx |W(r)| * g_R(r)e^{i\phi_w(r)}$ **(5)** and similarly for fat. The phase of the water and fat images are then demodulated from equation 5 using the low resolution estimates of the phase of the water and fat images ($\hat{\phi}_W(r)$, $\hat{\phi}_F(r)$). Finally, the water and fat images are calculated from the real part of the demodulated water and fat images, $|W(r)| \approx \mathrm{Re}\{\tilde{W}(r)e^{-i\hat{\phi}_w(r)}\} = \mathrm{Re}\{|W(r)| * g_R(r)e^{i\phi_w(r)}e^{-i\hat{\phi}_w(r)}\}$ **(6)** and similarly for fat. Extension to multi-coil is analogous to multi-coil IDEAL decomposition (3) and is omitted for brevity. Further decreases in scan time can be made by acquiring a low resolution image for one of the three echoes, in order to determine the field and phase maps. This approach is also omitted for brevity.

Methods: Scanning was performed at 1.5T and 3.0T (Signa TwinSpeed, VH/i respectively; GE Healthcare, Milwaukee, WI), using quadrature extremity coils (Medical Advances, Milwaukee, WI). All studies were approved by our IRB and informed consent was obtained. T2W IDEAL-FSE imaging was performed in the knee of 3 volunteers. FSE imaging parameters included: FOV=16cm, slice/gap=3.0/0.5, ETL=12, BW=±20kHz, TR/TE=5000/48, 22 coronal slices, 256x256 full resolution matrix, and 1 average. Non-contrast enhanced arteriographic imaging of the lower leg of 4th volunteer was performed at 3.0T using 3D-IDEAL-SSFP imaging (5). Imaging parameters included: BW=±100kHz, TR=4.7ms, TE=1.1/1.7/2.3ms, FOV_x=24cm, FOV_y=19.2cm, FOV_z=9.6cm with 256 x 204 x 96 matrix size for 0.9 x 0.9 x1.0mm^3 resolution. The fractional readout acquired 160 points. Reconstruction was performed with an off-line C program. To prevent ambiguities between assignment of water and fat within a calculated image, a "robust" reconstruction was combined with both the conventional iterative method and the proposed homodyne method (6).

Results: Fig. 1 shows calculated IDEAL water images obtained from a T2W FSE acquisition obtained in the coronal plane from a normal volunteer. Fig. 3a shows a full resolution image, while figs. 3b and 3c contain water images reconstructed after asymmetric removal of multiple k_y lines (echo fraction=0.625), using zero-filling (fig. 3b) and homodyne (fig. 3c). Fig. 2 contains maximum intensity projection (MIP) images of 3D non-contrast enhanced arteriographic IDEAL-SSFP images, reconstructed with zero-filling (2a) and the homodyne method (2b). Definite improvement in the sharpness of homodyne reconstructed images can be seen.

Discussion: In this work we have described a novel combination of conventional homodyne reconstruction with an iterative least squares water-fat separation algorithm, facilitating partial *k*-space acquisitions with maximized spatial resolution. *In vivo* images show improved resolution over simple zero-filling of unsampled areas of *k*-space, and demonstrate very similar image quality to full *k*-space acquisitions. The ability to reconstruct full resolution images from partial k_y or k_z data sets will allow for substantial decreases in overall scan time. Typical k-space fractions are 0.55-0.65, providing a 40% decrease in the minimum scan time with minimal compromise in image quality. Partial k_x acquisitions are beneficial for short TR sequences such as SSFP and SPGR, and could also be used to minimize first moment phase shifts and T2* signal losses. Maintaining a short TR is particularly important for SSFP to reduce banding artifacts caused by local field inhomogeneities.

Conclusion: This work has demonstrated the successful implementation of partial *k*-space reconstruction methods in combination with IDEAL water-fat separation. This approach will improve spatial resolution of images generated by water-fat decomposition methods that have previously relied on simple zero-filling. This will facilitate the use of partial readout methods used to obtain short TR and TE, as well as partial k_y and k_z methods used to reduce total scan time by reducing the number of k-space lines collected.

References: **1.** W Dixon, Radiology 1984 **2.** DC Noll et al, IEEE TMI, 1991 **3.** SB Reeder et al, MRM, 2003 **4.** SB Reeder et al, MRM *in press*. **5.** JH Brittain et al, ISMRM 2004, p. 12 **6.** H. Yu et al, ISMRM 2004, p. 345

Acknowledgments: The authors wish to thank Dwight Nishinura, PhD and John Pauly, PhD for helpful discussion.